Bulletin of the Seismological Society of America, Vol. 75, No. 1, pp. 175–191, February 1985

A SEISMIC-REFRACTION PROFILE ACROSS THE SAN ANDREAS, SARGENT, AND CALAVERAS FAULTS, WEST-CENTRAL CALIFORNIA

By Walter D. Mooney and Robert H. Colburn

Abstract

In 1981, the United States Geological Survey recorded a seismic-refraction profile across the southern Santa Cruz Mountains in west-central California to examine the shallow velocity structure of this seismogenic region. This 40-km-long profile, which consisted of three shotpoints, extended northeastward from near Watsonville, California, to Coyote Lake, crossing the San Andreas, Sargent, and Calaveras faults. This entire region is characterized by a highly heterogeneous upper crust. West of Watsonville, 1 km of alluvium with a velocity of 2.12 km/sec overlies a basement with a velocity 5.45 km/sec. The abrupt deepening of basement by 1.5 km just east of Watsonville at a subsurface fault suggests that the Zayante fault to the north and the Vergeles fault to the south are connected. The Tertiary sediment at the San Andreas fault is 2.5 km thick and has a velocity of 3.34 km/sec. The San Andreas fault is not marked by any distinctive seismic velocity features, whereas a 1-km-wide low velocity zone is found at both the Sargent and Calaveras faults. East of the Sargent fault, the basement surface forms a broad anticlinal structure, with velocities ranging from 5.4 to 6.0 km/sec. From the anticlinal crest, basement dips to the east beneath the Santa Clara Valley and reaches a maximum depth of 1 km on the east side; the overlying alluvium has a velocity of 2.7 km/sec. At the crest of the basement anticlinal structure, a vertical low-velocity zone coincident with exposed serpentine provides strong evidence of faulting.

Introduction

Geophysical studies of the upper crustal structure of west-central California are important for the further understanding of the geologic structure and tectonics in this seismically active region. The portions of the San Andreas, Sargent and Calaveras faults at the latitude of the city of Gilroy (Figure 1) were chosen as the site of a 1981 seismic-refraction investigation for two reasons. First, the region is of considerable geologic interest because it includes the "wedge" formed by the bifurcation of the San Andreas fault system south of Hollister (Figure 1). Thus, a determination of the two-dimensional structure and subsurface composition of crustal materials in the region is an important step in the reconstruction of the Cenozoic tectonics of central California. Second, the region lies along a portion of the San Andreas fault where a secondary fault, the Sargent fault, interacts with the San Andreas fault. Several studies of the seismicity and tectonics of this portion of the fault are currently underway (e.g., Bakun and McLaren, 1984). Detailed crustal velocity information is needed to determine the change in geologic units across the faults and to obtain more accurate hypocentral locations. We describe here the interpretation of the compressional-wave velocity structure in this area based on data from a 40-km-long east-west seismic refraction profile.

Geologic Setting

The study area traverses a complex geologic setting which includes three major faults: the San Andreas, Sargent, and Calaveras faults. From west to east, the profile extends from the Watsonville Valley (a northern extension of the Salinas

Valley), across the Santa Cruz Mountains and the Santa Clara Valley, to the westernmost flank of the Diablo Range (Figure 2). The profile follows California State Highway 152 from about 1 km northeast of Watsonville to about 4 km west of Gilroy. The west end of the profile traverses Quaternary alluvium of the Watsonville Valley. Tertiary sedimentary rocks are exposed east of Watsonville Valley as far as the Sargent fault (Figure 2). East of this fault, in the southern Santa Cruz Mountains, graywackes, greenstones, and associated serpentine and other ultramafic rocks of the Franciscan assemblage predominate (Bailey *et al.*, 1964, 1970),

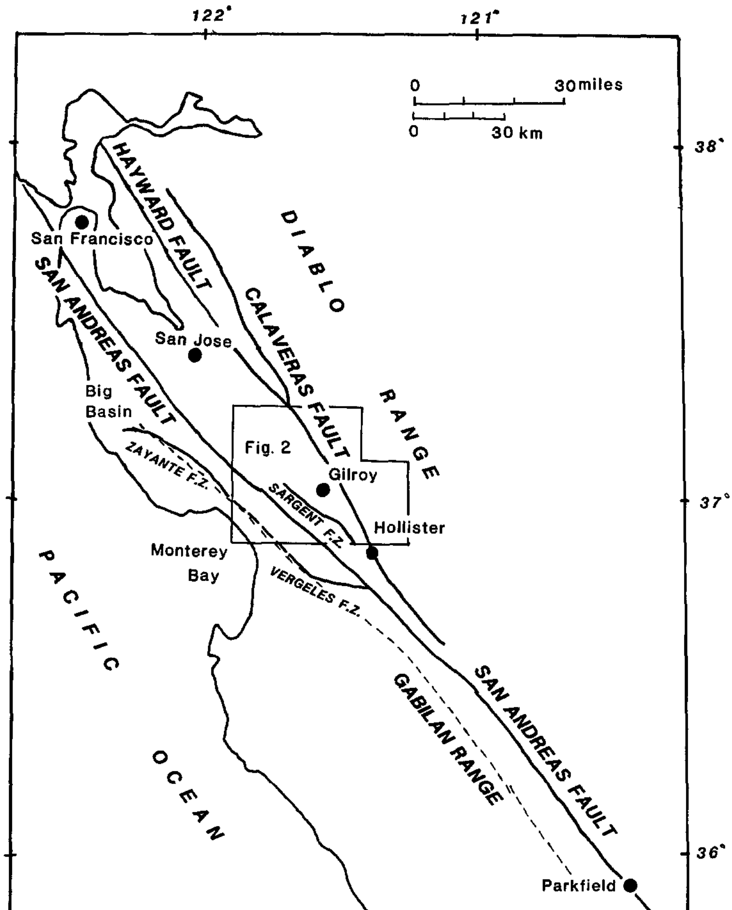

FIG. 1. Location map of central California showing relation of study area to local faults. Previous refraction profile from Big Basin to west of Parkfield analyzed by Walter and Mooney (1982) is shown (dashed line).

although some surficial Tertiary marine rocks are also present. Our line crosses the Berrocal fault about 6 km east of the Sargent fault (Rogers, 1966).

The eastern third of the profile crosses the central Santa Clara Valley, a fertile valley approximately 6 km in width at the latitude of the profile. Quaternary sediments, and the Cretaceous marine sediments of the Great Valley sequence are exposed to the east of the Santa Clara Valley (Dibblee, 1973; Rogers, 1966). The Calaveras fault zone cuts these units (Figure 2). The profile extends as far east as the edge of the Franciscan assemblage of the Diablo Range.

The portion of the profile between the San Andreas and Sargent faults is the most elevated of the profile, reaching a maximum elevation of 400 m above sea level. The western shotpoint (SP 3) is within the alluvium of the Watsonville Valley, the middle shotpoint (SP 2) is directly within the Sargent fault zone, and the eastern shotpoint (SP 1) is 1 km east of the Calaveras fault, in Great Valley sequence rocks.

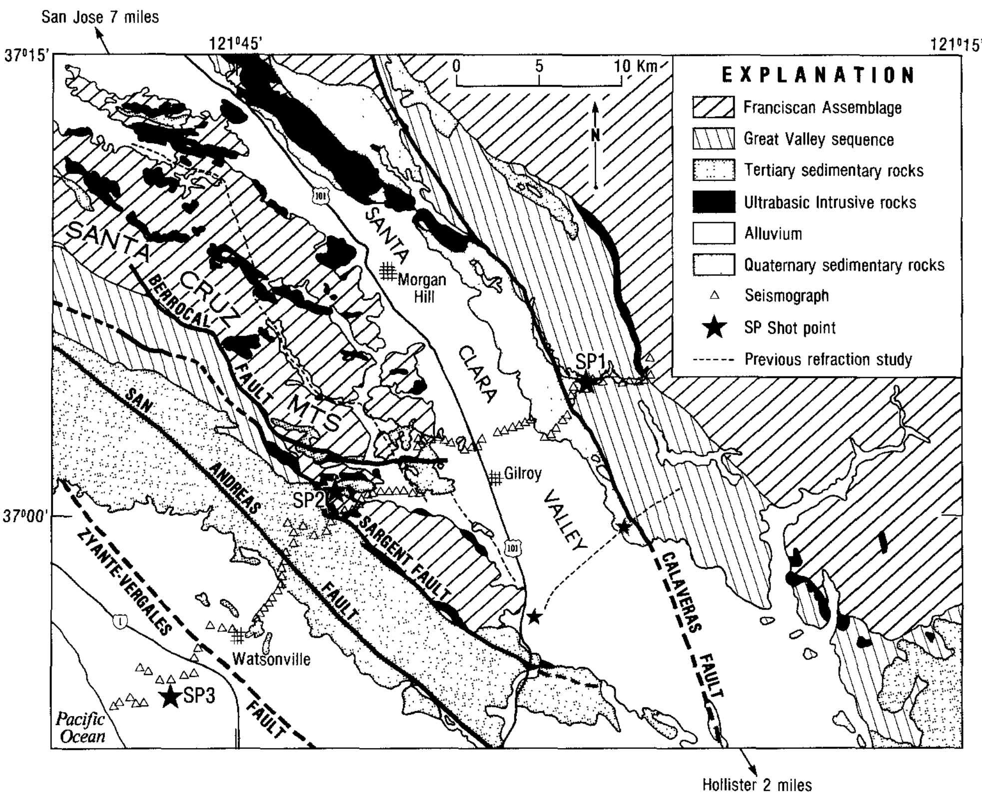

FIG. 2. Geologic map of study area with shotpoint and portable seismograph location. Generalized from Jennings and Strand (1958) and Rogers (1966). Location of previous refraction study by Mooney and Luetgert (1982) is shown.

Previous Seismic Work

Three seismic refraction profiles have previously been conducted in this area. Walter and Mooney (1982) interpreted a northwest-southeast trending profile on the western end of our profile extending from Big Basin in the Santa Cruz Mountains to the southernmost exposure of granites west of Parkfield in the Gabilan Range (Figure 1). In the Watsonville Valley, their interpretation shows a sediment thickness of about 1.5 km and a basement velocity of 5.45 ± 0.25 km/sec. The upper crustal velocity reaches 6.0 km/sec at a depth of 5 km.

Mooney and Luetgert (1982) presented models for a 15-long reversed profile recorded across the Santa Clara Valley and a 38-km-long unreversed profile in the southeastern Santa Cruz Mountains which crosses our profile (Figure 2). The reversed profile, located approximately 6 km south of our profile, showed an eastward thickening of the sedimentary fill of the Santa Clara Valley and revealed a high velocity (6.0 km/sec) basement layer that was interpreted to consist largely of Franciscan meta-volcanic rocks. In addition, a vertical low-velocity zone (2.7 km/

sec) was interpreted as extending to a depth of several kilometers at the Calaveras fault zone. The unreversed profile indicated that the 6.0 km/sec basement layer was also present in the southeastern Santa Cruz Mountains just west of the valley.

Blümling *et al.* (1985) interpreted a reversed seismic refraction profile that was placed directly along the Calaveras fault zone in the immediate area of shotpoint 1 (Figure 2). Where it crosses our profile their model shows surficial velocities between 2.6 and 4.5 km/sec overlying a seismic basement with a velocity of 5.7 km/sec at a depth of 4.5 km.

Given this previous work, our major interpretation problem concerned the velocity structure within 10 km on either side of the Sargent fault.

Field Procedure

The total profile length is approximately 40 km. The three shotpoints are located near each end of the profile and in the middle of the line. All three shots consisted of 700 kg of ammonium nitrate detonated in drill holes 45 m deep. The data were recorded on 100 portable cassette-recording seismographs which employ 2-Hz vertical component geophones (Healy *et al.*, 1982). The seismic signal is recorded in FM format at three separate gain levels, allowing for on-scale recording of seismograms at distances greater than 3 km from each shot (except for some clipped records west of the middle shotpoint). The seismographs' chronometers can be checked against a master clock system, providing an accuracy of better than 0.01 sec. Available roads allowed for a nearly linear profile, except for an offset 5 km west of Gilroy (Figure 2). All stations were located using 1:24,000 topographic maps to an accuracy of 15 m. The average station spacing along the profile is 580 m. Station and shotpoint locations are listed in Table 1.

Data Analysis

The data from all three shotpoints are shown in Figure 3. Impulsive first arrivals are visible on the majority of the records. Of the more than 200 seismograms, the uncertainty of the first arrival time was greater than 0.02 sec for only 14 records (mostly the seismograms distant from SP 1). We have listed in Table 2 the travel times of all first arrivals at each station, as well as distances between stations and shotpoints. Secondary arrivals from the deeper crust are visible beyond 30 km at a reduced time of 1.8 sec for the two end shotpoints (Figure 3). The data are presented at a reduction velocity of 6.0 km/sec with the first 3 sec of data shown.

The first arrivals for all three shots, the topography and surficial geology, and the uppermost portion of the final interpreted crustal structure are shown together in Figure 4 so that the relationship among them may be seen. The final model was obtained using standard travel-time methods, including two-dimensional computer raytracing (Červený *et al.*, 1977). Seismic amplitudes have not been modeled quantitatively. Because of the complexity of the geology along the line, the interpreted structure has been derived with particular attention to the constraints provided by previous refraction profiles and by the available geologic mapping.

In presenting our interpretation, we will discuss first the eastern half of the profile (between SP 1 and SP 2), then the western half (between SP 2 and SP 3), and finally, the combined east-west structure along the entire profile. Reference is made to the travel-time curves of Figure 4A. In discussing velocities and structure, the term "basement" refers to "seismic basement" which is defined here as the horizon with a velocity greater than 5.0 km/sec. The nomenclature of the profiles

TABLE 1

SHOTPOINT AND SEISMIC RECORDER LOCATIONS FOR THIS EXPERIMENT*

Shot Point Locations

Shot Point No.	Latitude (deg min sec)	Longitude (deg min sec)	Elevation
1	37 4 8.8	121 30 39.2	355
2	37 0 25.3	121 41 8.9	215
3	36 54 0.7	121 48 1.2	20

Seismic Recorder Locations

Location No.	Latitude (deg min sec)	Longitude (deg min sec)	Elevation
101	36 54 0.7	121 48 1.2	20
102	36 53 49.6	121 50 3.6	20
103	36 53 57.2	121 49 49.5	30
104	36 54 6.4	121 49 22.8	50
105	36 53 54.1	121 49 10.1	35
106	36 53 56.3	121 48 49.9	35
107	36 55 4.2	121 48 59.4	50
108	36 54 57.6	121 48 39.5	45
109	36 54 40.8	121 48 9.5	5
110	36 54 42.3	121 47 43.9	5
111	36 54 50.1	121 47 11.1	5
112	36 54 54.5	121 46 46.2	5
113	36 55 25.1	121 46 46.7	20
114	36 55 43.4	121 46 36.2	25
115	36 56 26.6	121 46 6.4	35
116	36 56 20.6	121 45 37.5	30
117	36 56 18.5	121 45 13.2	25
118	36 56 38.9	121 44 13.4	20
119	36 45 7.4	121 35 42.4	215
120	36 45 7.4	121 35 42.4	215
121	36 56 39.7	121 44 13.1	20
122	36 56 50.6	121 44 4.8	30
123	36 57 1.3	121 43 55.0	35
124	36 57 11.5	121 43 44.2	45
125	36 57 21.9	121 43 36.8	50
126	36 57 35.5	121 43 21.5	60
127	36 57 47.7	121 43 14.3	75
128	36 58 2.1	121 43 14.1	95
129	36 58 19.4	121 43 12.2	140
130	36 58 32.8	121 43 4.7	165
131	36 58 49.8	121 43 2.4	245
132	36 59 6.2	121 42 45.1	285
133	36 59 26.5	121 42 44.1	355
134	36 59 45.5	121 42 58.0	400
135	36 59 40.3	121 42 19.7	330
136	36 59 23.0	121 41 52.2	270
137	36 59 30.1	121 41 21.1	215
138	36 59 47.3	121 41 10.4	175
139	37 0 9.5	121 41 1.2	160
140	37 0 25.8	121 40 56.2	160
141	37 0 12.3	121 40 37.4	145
142	37 0 11.7	121 40 18.4	135
143	37 0 22.2	121 40 1.9	120
144	37 0 32.7	121 39 54.9	110
145	37 0 41.7	121 39 39.1	110
146	37 0 44.5	121 39 25.8	110

TABLE 1—*Continued*

Seismic Recorder Locations			
Location No.	Latitude (deg min sec)	Longitude (deg min sec)	Elevation
147	37 0 48.8	121 39 7.6	100
148	37 0 48.3	121 38 47.8	95
149	37 0 48.6	121 38 30.2	95
150	37 0 49.0	121 38 11.0	85
151	37 0 45.2	121 37 49.4	75
152	37 0 45.5	121 37 32.0	90
153	37 1 41.0	121 38 10.8	90
154	37 2 15.8	121 37 35.3	105
155	37 2 30.8	121 37 33.8	105
156	37 2 26.4	121 37 20.8	80
157	37 2 27.1	121 37 3.3	95
158	37 2 32.7	121 36 43.4	90
159	37 2 27.0	121 36 27.3	75
160	37 2 22.8	121 36 13.1	70
161	37 4 26.8	121 30 21.5	245
162	37 4 22.5	121 29 54.9	245
163	37 4 36.7	121 29 45.6	245
164	37 4 37.7	121 29 28.8	245
165	37 4 20.3	121 29 5.7	255
166	37 4 21.7	121 28 47.8	255
167	37 4 20.9	121 28 26.3	260
168	37 4 24.1	121 28 11.2	260
169	37 4 34.9	121 27 57.1	260
170	37 5 7.9	121 27 58.2	270
171	37 23 21.8	121 28 38.4	645
172	37 24 32.1	121 24 27.0	400
173	37 26 38.6	121 17 32.4	200
174	37 28 33.0	121 13 36.0	105
175	37 40 44.0	120 21 39.1	295
177	37 42 3.9	120 17 38.8	430
178	37 42 14.4	120 14 58.7	280
179	37 42 35.6	120 13 0.9	455
180	37 44 2.8	120 9 44.6	895
181	37 2 8.9	121 35 39.4	65
182	37 2 13.3	121 35 22.7	65
183	37 2 16.6	121 35 7.0	65
184	37 2 32.3	121 34 55.5	70
185	37 2 44.3	121 34 15.2	70
186	37 2 46.8	121 34 0.6	65
187	37 2 52.6	121 33 39.6	65
188	37 2 56.9	121 33 22.8	70
189	37 3 2.1	121 33 8.3	70
190	37 3 6.4	121 32 55.9	80
191	37 2 33.4	121 32 20.9	75
192	37 2 38.1	121 32 5.7	85
193	37 2 51.1	121 31 51.8	105
194	37 3 5.7	121 31 36.0	115
195	37 3 16.5	121 31 24.7	150
196	37 3 24.3	121 31 10.7	170
197	37 3 54.5	121 31 14.8	270
198	37 4 12.3	121 31 7.0	280
199	37 4 26.9	121 30 54.5	270
200	37 4 8.3	121 30 40.1	355

* Each location is identified by a location number.

is by shotpoint (SP) and direction; thus, SP IW refers to the data from shotpoint 1 recorded to the west. Positive distances are measured to the east, negative to the west.

Eastern Half of Profile

The data between SP 1 and SP 2 are recorded in the southern Santa Cruz Mountains and the Santa Clara Valley (Figures 2 and 4B). The apparent velocities recorded on profile SP 1W are 2.7, 7.1, and 4.7 to 4.8 km/sec (Figure 4A). The 2.7 km/sec velocity results from arrivals propagating through the Calaveras fault low-velocity zone and the Santa Clara Valley alluvial fill. The thin 4.5 km/sec layer

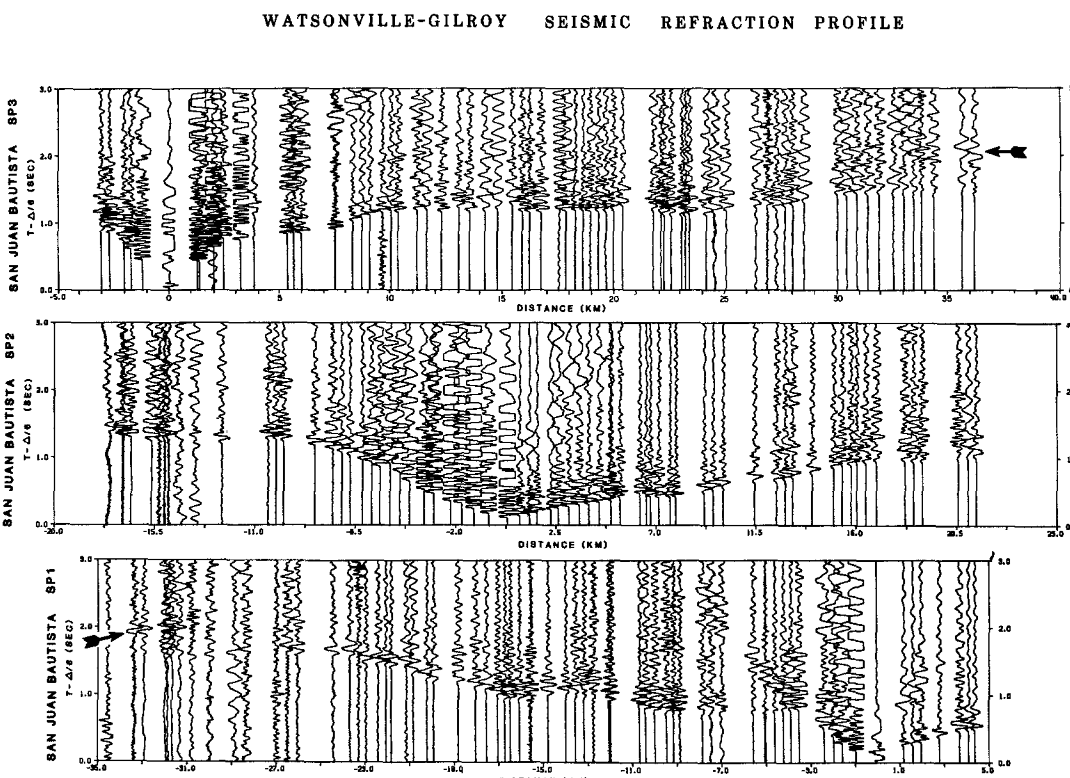

FIG. 3. Amplitude-normalized record sections for shotpoints (*bottom*) 1, (*middle*) 2, and (*top*) 3, with reduction velocity of 6.0 km/sec. First arrivals are clear; arrows at a distance of 36 km from shotpoint 3 and 34 km from shotpoint 1 indicate prominent secondary arrivals.

between the alluvium and basement shown in Figure 4C is based on the results of Mooney and Luetgert (1982). Closer spacing of instruments on our profile would be required for us to identify arrivals from this layer. At 8 km on SP 1W, the apparent velocity changes from 7.1 to 4.7 km/sec, and at 11 km there is a 0.1 see delay (Figure 4A), followed by an apparent velocity of 4.9 km/sec. The reversing data, profile SP 2E, show an apparent velocity of 4.5 km/sec to a distance of 7 km from SP 2, and a slight travel-time advance as the crossover to basement is reached (Figure 4A). The travel-time advance is followed at 8 km by an apparent velocity branch of 4.5 km/sec. An apparent velocity of 3.8 km/sec is observed crossing the Santa Clara Valley due to the thickening of the valley sediments and an apparent velocity of 5.5 km/sec is observed east of SP1.

TABLE 2

INITIAL ARRIVAL TIMES FOR EACH LOCATION*

Location No.	First Arrival Travel Times (reduced to 6.0 km/sec)					
	Shot Point 1		Shot Point 2		Shot Point 3	
	Distance	Travel Time	Distance	Travel Time	Distance	Travel Time
101	31.87	1.39	15.64	1.24	0.0001	0.02
102					3.05	0.87
103			17.58	1.34	2.69	0.86
104			16.90	0.93	2.03	0.75
105			16.95	1.32	1.72	0.62
106	32.93	1.52	16.55	1.29	1.21	0.46
107			15.28	1.24	2.43	0.77
108	31.66	1.50	15.04	1.28	1.99	0.64
109	31.32	1.50			1.25	0.47
110	30.77	1.47			1.35	0.43
111	29.97	1.55				
113			12.47	1.19	3.19	0.74
114					3.80	0.77
115			10.41	1.26	5.32	0.83
116	26.49	1.63	10.05	1.25	5.59	0.85
117	26.02	1.58	9.72	1.23	5.94	0.83
118			8.34	1.16	7.45	0.90
121			8.32	1.17	7.47	0.89
123	23.68	1.50	7.51	1.11	8.25	1.02
124			7.10	1.07	8.67	1.07
125	22.95	1.45	6.73	1.01	9.02	1.11
126	22.41	1.44	6.18	0.97	9.58	1.15
127	22.06	1.43	5.76	0.93	9.97	1.18
128	21.82	1.38	5.39	0.40	10.29	1.15
129			4.94	0.90		
130	21.14	1.40	4.50	0.78	11.14	1.18
131	20.84	1.26	4.07	0.65	11.58	1.20
132	20.22	1.14	3.41	0.52	12.24	1.15
133	19.92	1.12				
134			2.96	0.46	13.01	1.22
136	18.82	1.13	2.20	0.35	13.49	1.18
137	18.04	1.09	1.73	0.32	14.18	1.16
138	17.56	1.02	1.17	0.25	14.75	1.20
139	17.05	0.94	0.52	0.17	15.40	1.26
140	16.73	0.88	0.31	0.10	15.86	1.18
141	16.48	0.87	0.88	0.13		
142	16.07	0.88	1.32	0.15	16.18	1.16
143			1.66	0.18	16.70	1.15
145	14.79	0.92	2.28	0.23	17.52	1.20
146	14.46	0.61	2.62	0.26	17.82	1.17
147	13.99	0.97	3.09	0.27	18.24	1.19
148	13.56	0.89	3.56	0.29	18.58	1.17
149	13.17	0.89	3.99	0.30	18.91	1.16
150			4.46	0.33	19.28	1.14
151			4.97	0.37	19.61	1.15
152	11.97	0.86			19.95	1.17
153	12.05	0.89	4.98	0.44	20.36	1.25
154			6.28	0.48	21.74	1.16
155	10.68	0.79	6.58	0.46	22.09	1.15
156	10.41	0.72	6.76	0.42	22.22	1.10
157	9.99	0.70	7.14	0.41	22.55	1.09
158	9.47	0.69	7.65	0.42	23.03	1.08

TABLE 2—*Continued*

Location No.	First Arrival Travel Times (reduced to 6.0 km/sec)					
	Shot Point 1		Shot Point 2		Shot Point 3	
	Distance	Travel Time	Distance	Travel Time	Distance	Travel Time
159	9.15	0.68	7.91	0.41	23.20	1.08
160	8.87	0.66			23.37	1.11
161					32.55	1.39
162	1.17	0.20	18.19	0.93	33.00	1.40
163	1.58	0.27	18.58	0.93	33.44	1.38
164	1.95	0.30	18.97	0.93	33.80	1.46
166	2.78	0.37			34.35	1.38
168	3.69	0.46				
169	4.09	0.48			35.62	1.42
170	4.37	0.49			36.16	1.41
182	7.86	0.64	9.18	0.46	24.14	1.09
183	7.47	0.68	9.58	0.50	24.50	1.16
184	7.00	0.69	10.03	0.54	25.03	1.18
186	5.58	0.71	11.45	0.62	26.37	1.21
187	5.04	0.74			26.89	1.25
188	4.61	0.73	12.43	0.61	27.30	1.24
189	4.22	0.75			27.68	1.24
190	3.89	0.76	13.16	0.69	28.01	1.28
192	3.52	0.77	14.04	0.74	28.51	1.31
194	2.40	0.48	15.00	0.84		
195	1.97	0.38	15.37	0.87	30.02	1.41
196	1.58	0.27	15.78	0.88	30.44	1.40
197	0.98	0.17	16.04	0.90	30.90	1.42
198			16.44	0.92	31.38	1.43
199					31.89	1.44
200	0.03	0.02				

* Not all locations recorded all shots due to instrument failure or other problems (e.g., high cultural noise).

The upper crustal velocity model (Figure 4C) shows pronounced lateral variations along the profile. The velocity of basement between SP 1 and SP 2 varies from 6.0 to 5.45 km/sec, with a vertical low-velocity region of 4.0 km/sec material in between. There is a structural basement high at the western edge of the Santa Clara Valley. The 6.0 km/sec basement dips eastward toward the Calaveras fault, and the 5.45 km/sec material dips westward toward the Sargent fault (Figure 4C). This anticlinal structure is revealed by the dissimilar apparent velocities observed for the reversing shotpoints, and by the shape of the Santa Clara Valley as revealed by Mooney and Luetgert (1982).

The lateral variation in basement velocity is a feature of the crustal structure indicative of the geologic complexity of the region. Based on previous seismic refraction measurements in the Coast Ranges and on laboratory studies of Franciscan rocks (Stewart and Peselnick, 1977, 1978) we interpret the 6.0 km/sec rocks to be predominantly meta-volcanic rocks, the 4.0 km/sec rocks to be serpentine, and the 5.44 km/sec rocks to be meta-sedimentary rocks, all rock types associated with the Franciscan assemblage. The inferred serpentine body lies under the western edge of the Santa Clara Valley, between the Berrocal fault and an unnamed fault 3 km to the northeast (Dibblee, 1973; Rogers, 1966). The Berrocal fault is marked by serpentine outcrops along its length; we speculate that these migrated upward along the fault from our inferred body.

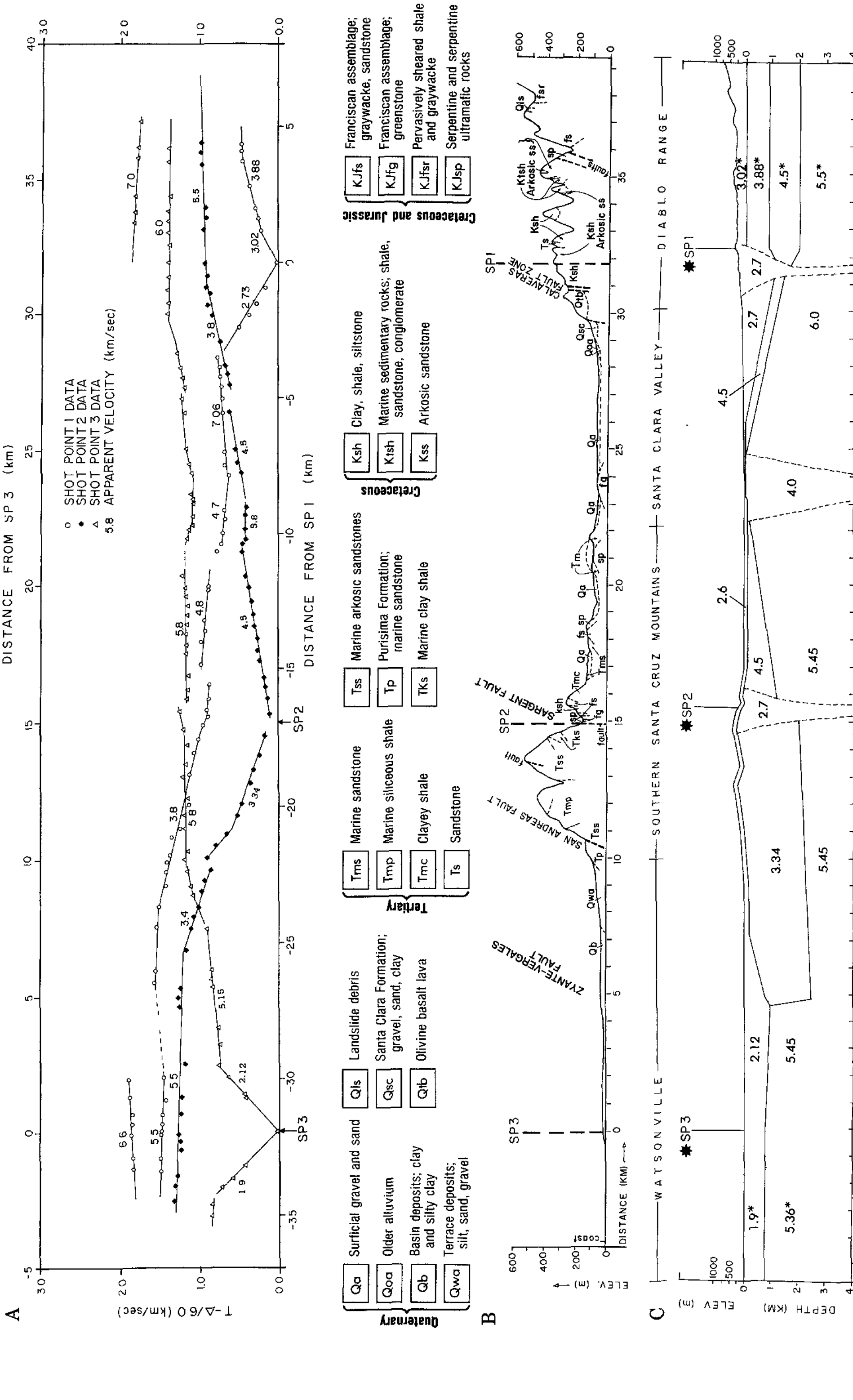

FIG. 4. (A) Observed travel-time curves from the three shotpoints; (B) geology and topography along the profile; and (C) interpreted velocity structure of the upper crust. Long dashed lines indicate fault zones.

A comparison between travel times calculated through our two-dimensional velocity model and our data show good agreement for the reversed profile between SP 1 and SP 2 (Figure 5). This model provided the best fit of travel-time curves to the data out of the several models derived. Calculations for a model without the 4.0 km/sec low-velocity zone resulted in significantly earlier arrival times despite attempts to minimize these. Another model we tested contains a near surface low-

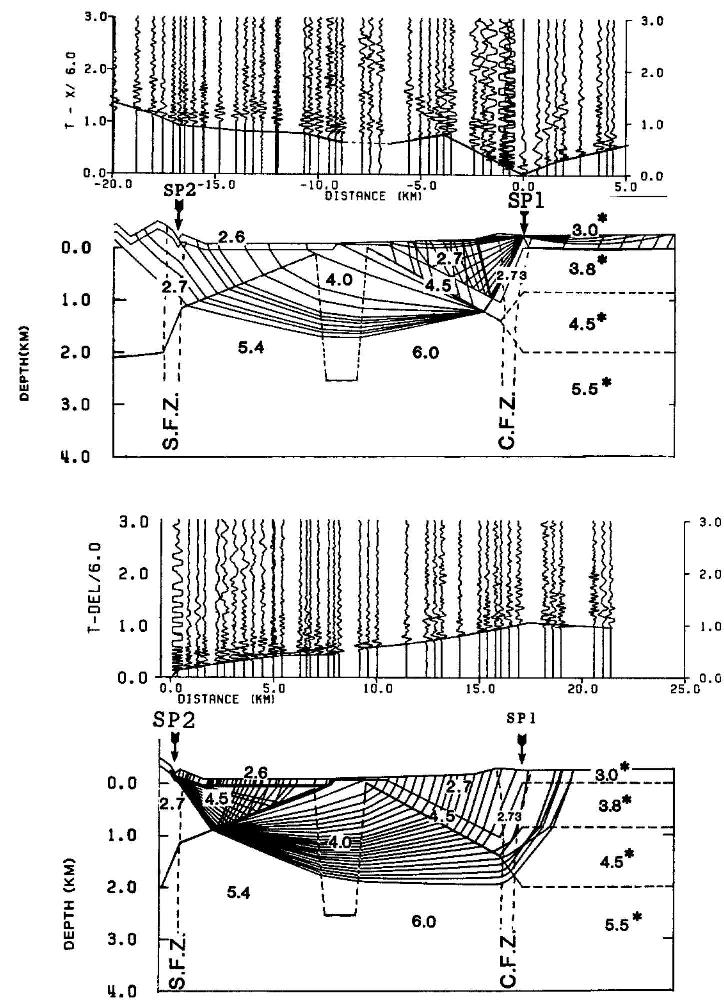

FIG. 5. East and west travel-time curves and ray trace diagrams east of SP 2. Numbers show velocities in kilometers/second; velocities marked by asterisks are unreversed. Sargent Fault Zone (S.F.Z.) and Calaveras Fault Zone (C.F.Z.) are indicated.

velocity zone for the first 7 km east of SP 2. This model provides a somewhat better fit to the delayed observed arrivals 15 km west of SP 1, but produces uniformly late arrivals for profile SP 2E. We note that some discrepancies between model travel times and observed travel times are expected as a lateral displacement of over 3 km occurs in the line at a distance of about 12 km west of SP 1 (Figure 2; Table 1). In an area of such geologic complexity, one can expect there will be significant changes in the observed travel-time curves for this large an offset. Further collection of seismic data are needed between SP 1 and SP 2 in order to place better defined constraints on our model.

The region east of SP 1 does not have reversed refraction coverage. Only apparent velocities for the three shots have been measured there. Profile SP 1E shows apparent velocities of 3.0 and 3.8 km/sec which are used as the two near-surface velocities. Profile SP 2E shows an apparent velocity of 5.5 km/sec which we have used as the fourth layer velocity. A layer with a velocity of 4.5 km/sec is included based on the results of Mooney and Luetgert (1982) and Blümling *et al.* (1985).

WESTERN HALF OF PROFILE

The region between SP 2 and SP 3 is another region where our refraction profile is reversed. Profile SP 2W shows a simple travel-time curve consisting of essentially two branches with apparent velocities of 3.1 to 3.4 km/sec and 5.8 km/sec (Figure 4A). The first branch corresponds to propagation in the Tertiary sediments west of the Sargent fault and the second branch is the basement refraction. The crossover distance between the apparent velocities is at about 8.5 km. The reversing profile, SP 3E, shows three apparent velocity branches in the first 15 km. The first branch, 2.12 km/sec, corresponds to arrivals traveling through the alluvium in the Watsonville area. The second, 5.15 km/sec, is a refraction along a slightly down-dipping basement that is calculated to have a true velocity of 5.45 km/sec. Beginning at about 7.5 km east of SP 3, a 0.2 sec travel-time delay occurs over a distance of 2.5 km. From 10 km east of SP 3 to SP 2, the apparent velocity is 5.8 km/sec. The travel-time observations between SP 2 and SP 3 are modeled by a velocity structure (Figure 4C) consisting of four layers with velocities of 2.12, 2.6, 3.34, and 5.45 km/sec. The 2.12 km/sec layer (layer 1), consisting of alluvium, pinches out to the east of a prominent basement fault. The 2.6 km/sec layer (layer 2) begins east of the prominent basement fault and consists of poorly consolidated sedimentary rocks and weathered Tertiary rocks. Layer 2 is underlain by layer 3, with a velocity of 3.34 km/sec consisting of consolidated Tertiary rocks. These Tertiary rocks are present east of the San Andreas fault, and reach a maximum thickness of 2.4 km at about 4.5 km west of the San Andreas fault. This point of maximum thickness corresponds to the down-dropped (eastern) side of the prominent basement fault.

This fault, occurring in a layer with a velocity of 5.45 km/sec, has a remarkably large 1.5 km vertical displacement making it one of the most significant features of the velocity structure along this profile. We interpret it to indicate that the Zayante fault to the north and the Vergeles fault to the south are connected by a buried fault, here referred to as the Zayante-Vergeles fault. This buried fault has a significant component of vertical displacement.

Travel-time curves and ray diagrams for the model between SP 2 and SP 3 are shown in Figure 6. The crustal velocity model provides an excellent fit both west and east of SP 3. However, on the reversed profile, at a distance of 8 to 15 km west of SP 2, the calculated travel-time curve is late by as much as 0.25 sec. An alternate model (indicated with a dotted line in Figure 8), which replaces part of the 2.12 km/sec region with the 3.34 km/sec velocity, reduces this descrepancy to 0.20 sec, but the calculated travel times for this alternate model are 0.18 sec early 6 km east of SP 3. Densely recorded refraction or seismic reflection data are needed to determine the detailed structure above the basement fault.

COMBINED EAST-WEST STRUCTURE

Longer range refraction data is provided by the reversal between SP 1 and SP 3. The ray trace diagrams and travel-time curves for these profiles are shown in Figure

7. Travel times through the composite crustal velocity model are in good agreement with the observed data. In the vicinity of SP 2, profile SP 1W shows a significant change in apparent velocity from 4.8 to 3.8 km/sec. This low apparent velocity is due to two abrupt changes that occur in the velocity structure upon crossing the Sargent fault (SP 2). First, the near-surface layer decreases in velocity from 4.5 to 3.34 km/sec at the Sargent fault, corresponding to the change from Franciscan rocks east of the fault to Tertiary marine rocks west of the fault. Second, there is

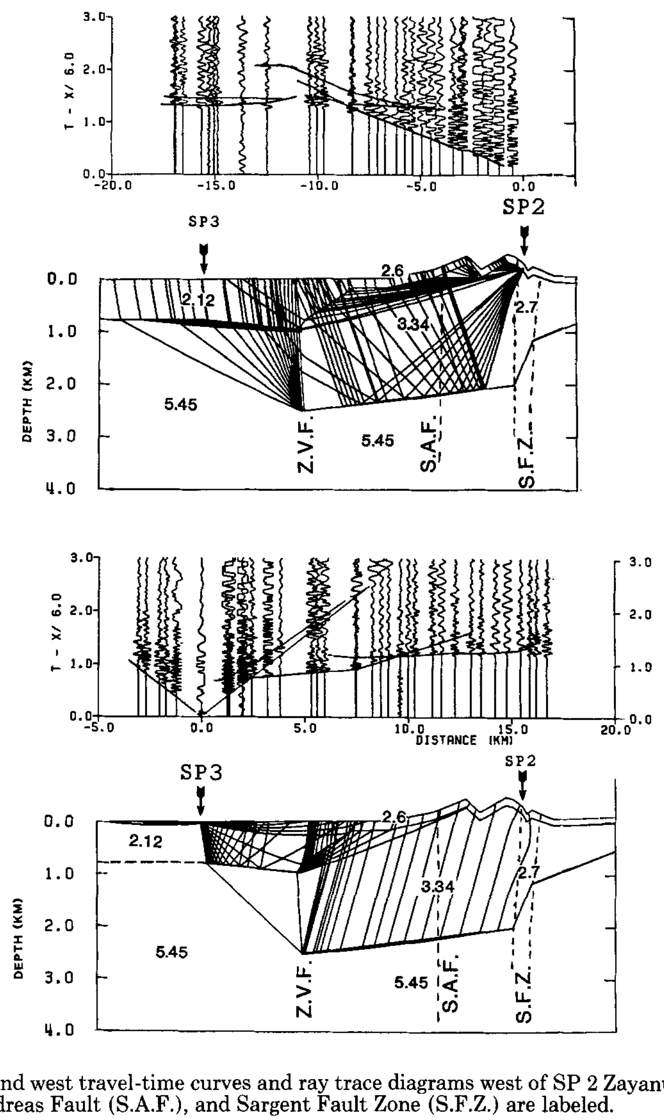

FIG. 6. East and west travel-time curves and ray trace diagrams west of SP 2 Zayante-Vergeles Fault (Z.V.F.), San Andreas Fault (S.A.F.), and Sargent Fault Zone (S.F.Z.) are labeled.

0.5 km vertical displacement in basement (down to the west) and a vertical, 1-km-wide low velocity zone across the Sargent fault. These features result in a significant delay in the arrival times. Beyond 30 km west of SP 1, there is a clear travel-time advance of 0.1 sec. This advance is due to the vertical displacement on the Zayante-Vergeles fault which we previously discussed.

The dashed line in Figure 7 at 4.0 km depth indicates a change in the velocity gradient; the average gradient for the model above 4.0 km is 0.03 km/sec/km, whereas below 4.0 km depth, the average gradient is 0.004 km/sec/km. We attribute this difference to the nearly complete closing of cracks by 4 km depth, below which the velocity gradient is very small (e.g., Lin and Wang, 1980).

As mentioned earlier, the data show clear secondary arrivals at the west end of the profile SP 1W (arrows in Figure 3; see also Figure 7). These arrivals are present, although not quite as distinct, on the reversed profile, SP 3E. We have modeled

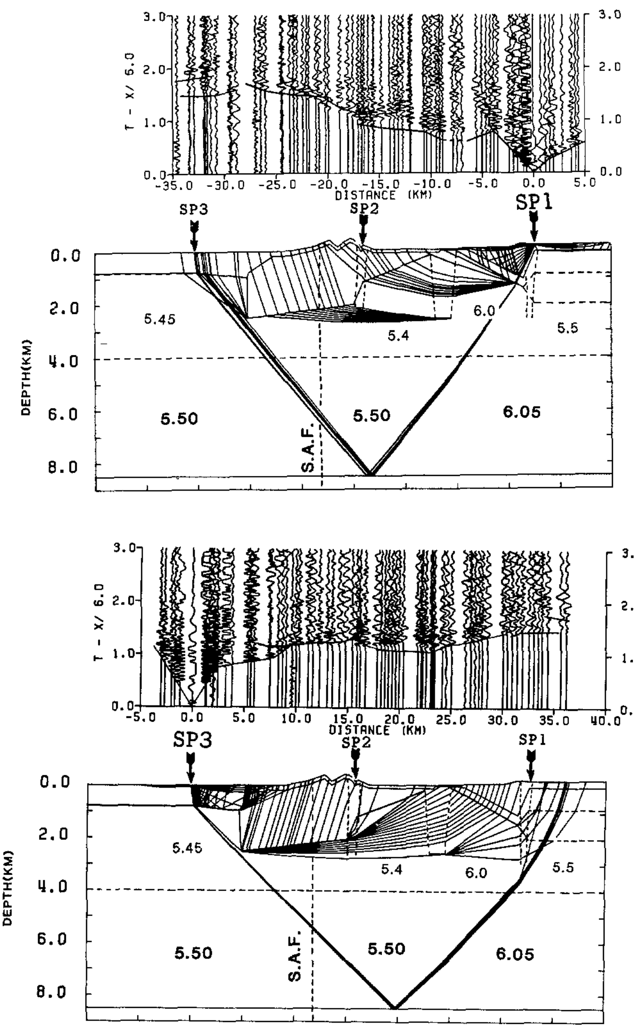

FIG. 7. Ray trace diagrams and travel-time curves for the model across the entire profile. San Andreas Fault (S.A.F.) is labeled.

these arrivals as reflections off a velocity discontinuity at 8.5 km depth. The model fits the arrivals at the west end of the profile, although the calculated arrivals at the east end are early by about 0.2 sec. The velocity below the discontinuity is unconstrained; however, for a ray to be critically reflected, we estimate that the velocity below this boundary must be about 6.3 to 6.4 km/sec.

Discussion and Conclusions

The interpretation of this profile has shown several important features of the upper crustal structure in west-central California. Our composite interpretation of the crustal structure is shown with a vertical exaggeration of 2:1 in Figure 8. We discuss the major features of this structure proceeding downward from the near-surface.

The alluvial fill of the Watsonville Valley amounts to 800 to 900 m. The low seismic velocity (2.12 km/sec) measured there indicates that well-consolidated sediments are either thin or absent in the upper 900 m. The Tertiary sediments of the western Santa Cruz Mountains are about 2.5 km thick and are characterized by a seismic velocity of 3.34 km/sec. This low velocity indicates that the sediments are not highly metamorphosed. The near-surface rocks of the Franciscan assemblage of the eastern Santa Cruz Mountains have a seismic velocity of 4.5 km/sec, essentially the same as that measured in the Fransiscan assemblage of the central Diablo Range (Walter and Mooney, 1982). At the easternmost flank of the Santa Cruz Mountains, a region of low seismic velocity (4.0 km/sec) extends to several

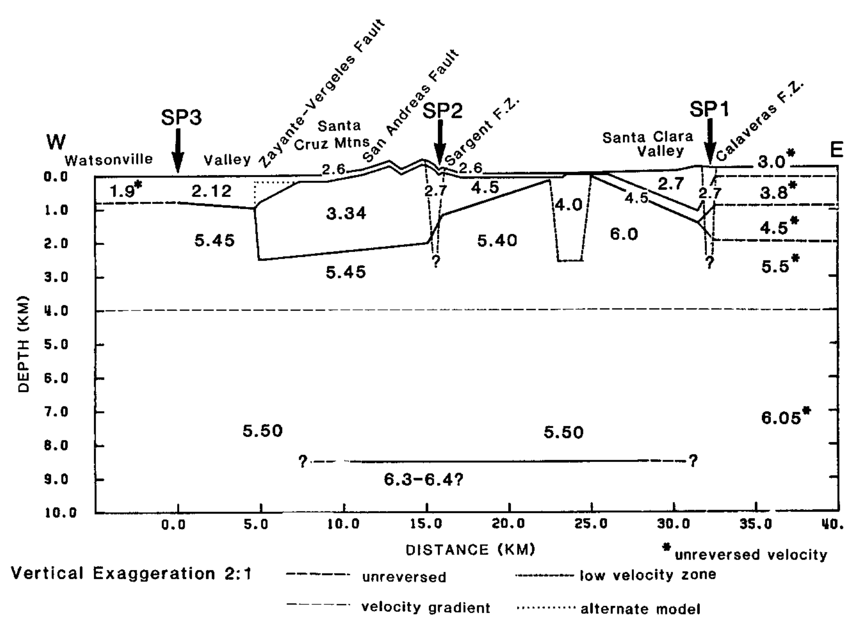

FIG. 8. Detailed model diagram, including deeper structure. Horizontal dashed line indicates a change in velocity gradient. Asterisks indicate unreversed velocities.

kilometers depth. Based on the surficial geology, we interpret this area to consist of sheared serpentine which migrated along steeply dipping faults within the Franciscan assemblage.

The alluvial fill of the Santa Clara Valley thickens to the east, reaching a maximum of 1.0 km at this latitude, as contrasted to a maximum fill of 1.5 km determined from the profile 6 km further south (Mooney and Luetgert, 1982). East of the Santa Clara Valley, rocks of the Great Valley sequence are exposed. These rocks show a sequence of apparent velocities of 3.0, 3.8, and 4.5 km/sec in the upper 2 km. True velocities were not determined in the present study but these velocities are consistent with the results of Blümling and others (1985) who analyzed a reversed seismic refraction profile which crosses our profile.

We define seismic basement as that horizon with a seismic velocity of 5.0 km/sec or greater. Several prominent structures are determined on this surface. A buried fault occurs beneath the Watsonville Valley, with a vertical displacement (down on the east) of about 1.5 km. Following earlier geologic inference (Jennings, 1977) we suggest that this fault connects the Zayante fault of the west-central Santa Cruz Mountains with the Vergeles fault of the Gabilan Range (Figure 1). In contrast to the large vertical offset on the Zayante-Vergeles fault, we observe no basement structural change across the San Andreas fault. The Sargent fault is marked by a 0.7 km rise (up to the east) on basement. In the area of the eastern Santa Cruz Mountains and Santa Clara Valley, the basement surface forms a broad anticlinal surface with a maximum relief of 1.3 km. The zone of 4.0 km/sec seismic velocity occurs at the center of this anticline. The depth to basement reaches 2 km east of the Calaveras fault.

The seismic velocity of basement is not constant along the profile. For much of the profile the velocity is 5.4 to 5.5 km/sec, however, the velocity is 6.0 km/sec beneath the Santa Clara Valley. A higher seismic velocity for the basement rocks of the valley, which has also been reported by Mooney and Luetgert (1982), suggests a distinct geologic composition for these rocks. Based on the geology of the southeastern Santa Cruz Mountains, and previous seismic refraction measurements in the Coast Ranges (Stewart, 1968; Walter and Mooney, 1982; Blümling and Prodehl, 1983) and laboratory studies of Franciscan rocks (Stewart and Peselnick, 1977, 1978), we interpret the 6.0 km/sec rocks to consist mainly of meta-volcanic rocks associated with the Franciscan assemblage. The remaining basement rocks, with seismic velocity 5.4 to 5.5 km/sec may consist of one of at least two rock types. At the shallow depths of the present measurements (1 to 3 km), both Franciscan assemblage metasediments and granitic rocks have seismic velocities in this range. Thus, we cannot define on the basis of seismic velocity alone where the basement rock type changes from the Franciscan assemblage of the eastern Santa Cruz Mountains to the granitic basement of the Watsonville Valley. The structure of the basement surface shows the largest changes at the Sargent and Zayante-Vergeles faults, rather than the San Andreas fault (Figure 8), which suggests that the basement change occurs at one of the former faults.

The seismic-refraction profile crosses four major faults, three of which have major structural features. The vertical offsets at the Zayante-Vergeles and Sargent faults have already been noted; the Calaveras fault also appears to correlate with a basement offset (down on the east) of about 0.5 km. The Calaveras fault also is marked by a change in basement velocity from 6.0 to 5.5 km/sec.

Based on travel-time delays, two faults, the Sargent and Calaveras, are interpreted to be characterized by seismic low-velocity zones. A low-velocity zone at the Calaveras fault is well documented (Meyer-Rosa, 1973; Mooney and Luetgert, 1982; Blümling *et al.*, 1984), but this is the first report of a low-velocity zone at the Sargent fault. The depth extent of the low-velocity zones is not well determined by the present seismic data, but our ray trace calculations indicate that the low-velocity zone extends into the basement rocks at a depth of 2 km and more.

The deeper crustal structure beneath the southern Santa Cruz Mountains includes a seismic discontinuity at 8 to 9 km depth. No determination has been made of the velocity below this discontinuity due to the short profile length. We assume that the velocity increases to 6.3 to 6.4 km/sec below this depth based on the deep structure of the neighboring areas (Walter and Mooney, 1982).

Acknowledgments

The field work for this study was performed by J. R. Van Schaack, E. E. Criley, G. A. Molina, V. D. Sutton, R. P. Meyer Jr., W. J. Lutter, A. W. Walter, S. K. Gallanthine, J. N. Roloff, and L. R. Hoffman.

K. W. Gortner collected geologic information along the profile. Geologic discussions with K. M. Williams were helpful. Critical reviews by S. W. Stewart, K. M. Williams, and J. J. Zucca are greatly appreciated. Comments by an anonymous reviewer improved the text.

REFERENCES

Bailey, E. H., W. P. Irwin, and D. L. Jones (1964). Franciscan and related rocks, and their significance in the geology of western California, *Calif. Div. Mines Geol. Bull.* **183,** 177 pp.

Bailey, E. H., M. C. Blake, and D. L. Jones (1970). On-land Mesozoic oceanic crust in California Coast Ranges, *U.S. Geol. Surv. Profess. Paper* 700-*C,* C70–C81.

Bakun, W. H. and M. McLaren (1984). Microearthquakes and the nature of the creeping-to-locked transition of the San Andreas fault zone near San Juan Bautista, California, *Bull. Seism. Soc. Am.* **74,** 235–254.

Blümling, P. and C. Prodehl (1985). Crustal structure beneath the eastern part of the Coast Ranges (Diablo Range) of central California from explosion seismic and near earthquake data, *Phys. Earth Planet. Interiors* **31,** 313–326.

Blümling, P., W. D. Mooney, and W. H. K. Lee (1984). Crustal structure of the southern Calaveras fault zone, central California, from seismic refraction investigations, *Bull. Seism. Soc. Am.* **75,** 193–209.

Červený, V., I. A. Moltokov, and I. Pšenčík (1977). *Ray Method in Seismology,* University of Karlova, Prague, Czeckoslovakia, 214 p.

Dibblee, T. W., Jr. (1973). Geological maps of the Morgan Hill, Mt. Madonna, Mt. Sizer, Gilroy Hot Springs, and Gilroy quadrangles, California, *U.S. Geol. Surv. Open-File Maps,* 1:24, 000.

Healy, J. H., W. D. Mooney, H. R. Blank, M. E. Gettings, W. M. Kohler, R. J. Lamson, and L. E. Leone (1982). Saudi Arabian seismic deep-refraction profile: Final Project Report, Saudi Arabian Deputy Ministry for Mineral Resources, *U.S. Geol Surv., Open-File Rept. 02-37,* 429 pp.

Jennings, C. W. (1977). Geologic Map of California, California Division of Mines and Geology, Sacramento, California, 1:750000.

Jennings, C. W. and R. G. Strand (1958). Geologic map of California, Santa Cruz sheet, California Division of Mines and Geology, Sacramento, California, 1:250,000.

Lin, W. and C. Y. Wang (1980). *P*-wave velocities in rocks at high pressure and temperature and the constitution of the central California crust, *Geophys. J.* **61,** 379–400.

Mayer-Rosa, D. (1973). Traveltime anomalies and distribution of earthquakes along the Calaveras fault zone, California, *Bull. Seism. Soc. Am.* **63,** 713–729.

Mooney, W. D. and J. H. Luetgert (1982). A seismic refraction study of the Santa Clara Valley and southern Santa Cruz Mountains, west-central California, *Bull. Seism. Soc. Am.* **72,** 901–909.

Rogers, T. H. (1966). Geological map of California, San Jose sheet, California Division of Mines and Geology, Sacramento, California, 1:250,000.

Stewart, S. W. (1968). Preliminary comparison of seismic traveltimes and inferred crustal structure adjacent to the San Andreas fault in the Diablo and Gabilan Ranges of central California, in *Proc. Conf. Geological Problems of San Andreas Fault System,* W. R. Dickinson and A. Granta, Editors, Stanford Univ. Publ. Geol. Sci. **11,** 218–230.

Stewart, R. and L. Peselnick (1977). Velocity of compressional waves in dry Franciscan rocks to 8 kolobars and 300°C, *J. Geophys. Res.* **82,** 2027–2039.

Stewart, R. and L. Peselnick (1978). Systematic behavior of compressional velocity in Franciscan rocks at high pressure and temperature, *J. Geophys. Res.* **83,** 831–839.

Walter, A. W. and W. D. Mooney (1982). Crustal structure of the Diablo and Gabilan Ranges, Central California: a reinterpretation of existing data, *Bull. Seism. Soc. Am.* **72,** 1567–1590.

U.S. GEOLOGICAL SURVEY
345 MIDDLEFIELD ROAD, MS 77
MENLO PARK, CALIFORNIA 94025

Manuscript received 15 March 1984